applied sciences

MDPI

Article

# Prediction Analysis of Surface Roughness of Aluminum Al6061 in End Milling CNC Machine Using Soft Computing Techniques

**Serge Balonji, Lagouge K. Tartibu * and Imhade P. Okokpujie**

Mechanical and Industrial Engineering Technology, University of Johannesburg, Johannesburg 2006, South Africa; balonjiserge@yahoo.com (S.B.); imhadeprincess@gmail.com (I.P.O.)
* Correspondence: ltartibu@uj.ac.za; Tel.: +27-11-559-6476

**Abstract:** Computer numerically controlled (CNC) milling has been one of the most commonly used manufacturing processes for the performance of multiple operations, from tiny integrated circuits to heavy-duty mining machine gearboxes. It is a well-known machining process that offers close tolerances and repeated operations. However, the choice of machining parameters to achieve a desired part's surface roughness (SR) remains a challenge. In the present study, artificial neural network (ANN) and adaptive network-based fuzzy inference system (ANFIS) approaches have been used to predict and monitor the surface roughness of aluminum Al6061 machined blocks. Furthermore, both models have been hybridized with genetic algorithm (GA) and particle swarm optimization (PSO) to investigate the potential enhancement in the prediction performance of the hybrid approach. The results show that factors such as the population size, the acceleration values, the choice of membership functions, and the number of neurons and layers significantly influence the prediction performance of the proposed models. Through a parametric analysis, this study demonstrates how the configuration of the models could affect the prediction performance. While exhibiting the impact of models' hyperparameter combination on the prediction ability, this study provides insight into the development of suitable prediction models and the potential of soft computing techniques to predict the surface roughness of aluminum Al6061 blocks on CNC machines.

**Keywords:** artificial neural network (ANN); adaptive network-based fuzzy inference system (ANFIS); genetic algorithm (GA); particle swarm optimization (PSO); ANN-PSO; ANN-GA; ANFIS-PSO; ANFIS-GA; aluminum Al6061; CNC machine



**Citation:** Balonji, S.; Tartibu, L.K.; Okokpujie, I.P. Prediction Analysis of Surface Roughness of Aluminum Al6061 in End Milling CNC Machine Using Soft Computing Techniques. *Appl. Sci.* **2023**, *13*, 4147. https://doi.org/10.3390/app13074147

Academic Editor: Panagiotis G. Asteris

Received: 7 March 2023
Revised: 19 March 2023
Accepted: 22 March 2023
Published: 24 March 2023



## 1. Introduction

Surface roughness is a surface irregularity with smaller intervals within the crest and bottom, unlike waviness. Roughness is a collection of true surface harshness, traditionally interpreted as a deviation of the measured form between a reference and the bounds of a length when waviness is ignored [1]. The true surface is referred to as the surface curbing the solid object configuration. It is a separate layer from the environment. The surface roughness profile is shown in Figure 1, where yi is the vertical distance from the mean line to a given data point along the profile line and l is the mean width of the profile line.

The surface roughness (SR) is expressed as a value in a mean arithmetical deviation Ra (Equation (1)) of the profile from the centerline average and Rmax (also called Rt or Rtotal), which is the height from the lowest point to the highest peak. It is expressed mathematically as follows:

$$\mathrm{Ra} = \frac{1}{L}\int_0^L |y(x)|dx \quad (1)$$

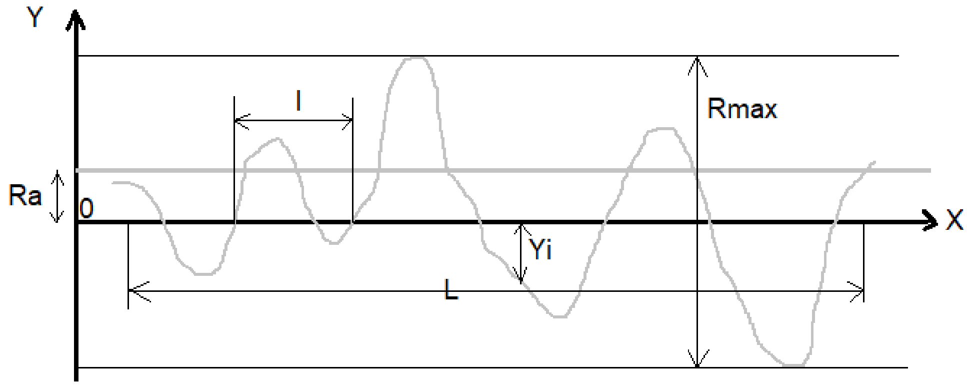


**Figure 1.** Surface roughness profile: yi is the vertical distance from the mean line to a given data point along the profile line; l is the mean width of the profile line.

where y represents the absolute values of distances between profile points and the centerline along a length L of the measured surface. The surface roughness is at the center of the interaction between an object and elements in its proximity. For this reason, its value is of major concern in the manufacturing process. The surface finish in contact with other components significantly affects friction, wear, and component life. When manufacturing a workpiece, caution is required to set the surface roughness within the recommended range in terms of Ra and Rt. Two common methods are used to measure the surface roughness, namely the contact and non-contact methods. The contact method includes a stylus profilometer and a white light interferometer [2], while the non-contact method includes the use of a Focus Variation Microscope [3]. In the present study, the experimental results were measured using a Mitutoyo surface roughness tester and Press o-firm [4].

As for milling machining, several factors may affect the surface roughness. These include, but are not limited to, the following:

- Cutting parameters: feed rate and spindle speed;
- Depth of cut: radial and axial depths;
- Tool configuration: insert geometry, insert materials, tool length;
- Machining condition: method of lubrication;
- The rigidity of the machine, tool, and workpiece;
- and the workpiece's raw material.

Researchers have employed one or a combination of the above factors to study their influence on the surface roughness. SI Wang et al. [5] considered the effect of the cutting parameters, tool geometry, and tool interference, as well as the tool–workpiece relative movement, on surface generation to devise a 3D surface topography simulation model for ultra-precision raster milling processes.

In order to achieve an optimum or at least more acceptable machining result that meets a work requirement, several approaches have been proposed to predict the surface roughness from selected variables that influence the surface texture of a workpiece in the end-milling machining process. Trial-and-error, empirical, and analytical methods were the earliest methodologies to predict surface roughness. Researchers used empirical methods to test a set of findings that were supported by experimental evidence. Analytical approaches are frequently used to solve equations for specific parameter circumstances [6]. However, empirical models are frequently developed by regression analysis of practical experiments [7].

Okokpujie and Okonkwo [4] explored the effects of four cutting parameters on the machined surface of Al 6061 alloy under minimum quantity lubricant (MQL) conditions. The study used a numerical statistical method. The surface roughness was predicted with accuracy of 89.5%. Furthermore, their study reveals a link between input factors (spindle rotational speed, axial depth of cut, radial depth of cut, and feed rate) and output variables (surface roughness obtained by CNC milling an alloy AI6061).

Although empirical and analytical techniques are suitable for the modeling and the analysis of the surface roughness, they have the following limitations [8,9]:

- Empirical and analytical approaches are time-consuming, especially when a large amount of data is required for analysis;
- Because the amount of data used for the analysis is significant, building models using these traditional approaches is relatively more challenging;
- Because there are so many variables to consider, the experiment is susceptible to failure to generate the expected findings.

ANN is a computing system composed of a collection of connected nodes emulating neurons in the human brain and capable of solving problems such as function approximation, classification, and time-series prediction. The ANN approach has lately gained researchers' interest in addressing and modeling complicated issues and dealing with nonlinearity between parameters in various fields. It is a multilayer network in which every neuron in one layer is fully linked to every neuron in the layer above it. Figure 2 depicts a typical ANN arrangement.

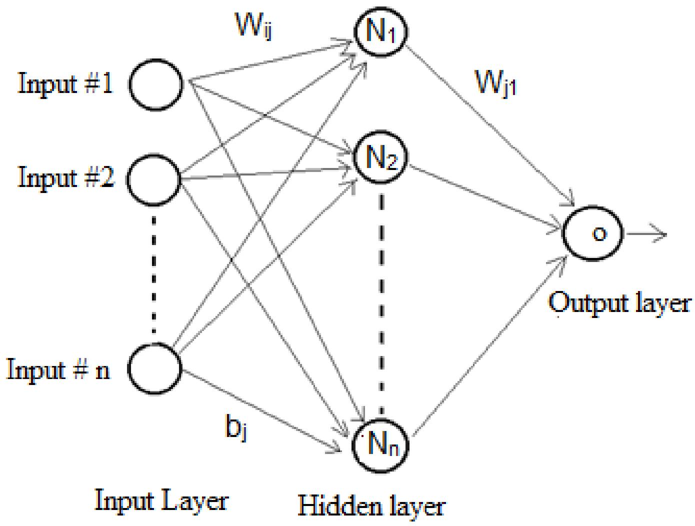


**Figure 2.** Artificial neural network structure.

Various researchers have used the ANN approach to predict the surface roughness of machined components: Cem Boga and Tahsin Koroglu [10] investigated the impact of machining parameters on the surface roughness of a high-strength carbon fiber composite plate using ANN. The analysis showed that the cutting tool and the feed rate have a stronger impact on the surface roughness than the spindle speed. As for ANN settings, the authors chose feedforward backpropagation as the model architecture because of its popular application. Deshpande et al. [11] used the ANN approach to analyze the turning operation and predict the surface roughness of an Inconel 718. Data were obtained from the machining of the Inconel 718 using cryogenically treated and untreated inserts. The surface roughness was predicted with 98% accuracy. According to the study, the ANN model is more reliable than the regression-based models in predicting Inconel 718's surface roughness in the turning operation.

The ANN parameters can be altered to allow better combinations for the model's improvement.

S. Karabulut [12] used uncoated carbide composites to produce AA7039/Al2O3 metal matrix composites and examined the impact of milling settings on the surface roughness and cutting force using a neural network and the Taguchi method. The Levenberg–Marquardt and the backpropagation algorithms were used to achieve better results. Furthermore, D. Baptista and Batista D. [13] pointed out that the Levenberg–Marquardt method, which converges more frequently and speeds up training, is acknowledged as having substantially superior performance than backpropagation, which is likely the most widely used ANN algorithm. S.O. Sada and S.C. Ikpeseni [14] compared the performance of ANN and ANFIS in predicting the machining response (metal removal and tool wear). They conducted hyperparametric evaluation by modifying learning algorithms (Levenberg–Marquardt, scalar conjugate gradient, and resilient backpropagation) and activation functions (logsig, tangsig, and purelin), and a range of neurons (2–20) were assessed to find the most effective one to perform training, validation, and testing. According to Haykin [15], the complexity of the system being modeled determines how many neurons are needed in the hidden layer. A. Yeganefar et al. [16] predicted and optimized the surface roughness and cutting forces in the slot milling of aluminum alloy 7075-T6 using ANN and a multi-objective genetic algorithm. Machining parameters included the cutting speed, feed per tooth, depth of cut, and tool type. Hyperparameters were fine-tuned and the Levenberg–Marquardt and RMSprop algorithms were chosen to train the model. Furthermore, the authors considered one or two hidden layers, as, if more are used, this can lead to a high prediction error.

Although ANN is more efficient and accurate than mathematical models, numerous research works have highlighted ANN's limitations, such as becoming trapped in local vertices and showing constraints to cross-peaks in the error function range. Shain M.A. et al. [17] pointed out that ANN has limitations in geotechnical domains. The inability to extract information from trained neural networks and forecast outside the range of training data are two of these constraints. Several researchers have proposed ANN hybridization with other optimization models to enhance the computing ability of ANN [18].

The adaptive network-based fuzzy inference system (ANFIS) is a neural network based on the Takagi–Sugeno fuzzy inference system. It offers the possibility to harness the benefits of pairing neural networks and fuzzy logic principles in a single structure, since it incorporates both. Its inference system comprises a collection of fuzzy IF-THEN rules with the capacity to approximate nonlinear equations through learning and forecasting disordered time series. Various types of fuzzy inference systems have been identified in the literature. They may be divided into three types, described in detail by Jang [19]. Figure 3 depicts a two-input type 3 fuzzy inference system construction with five layers separated. Input variables are represented by x and y; layer 1 has square nodes, which are labeled A for input x and B for input y; layer 2 has circled nodes, which are labeled Π; layer 3 has circled nodes, which are labeled N; layer 4 has square nodes, which are labeled 1–9; and layer 5, the sum of all incoming signals, has a circled node that is labeled Σ.

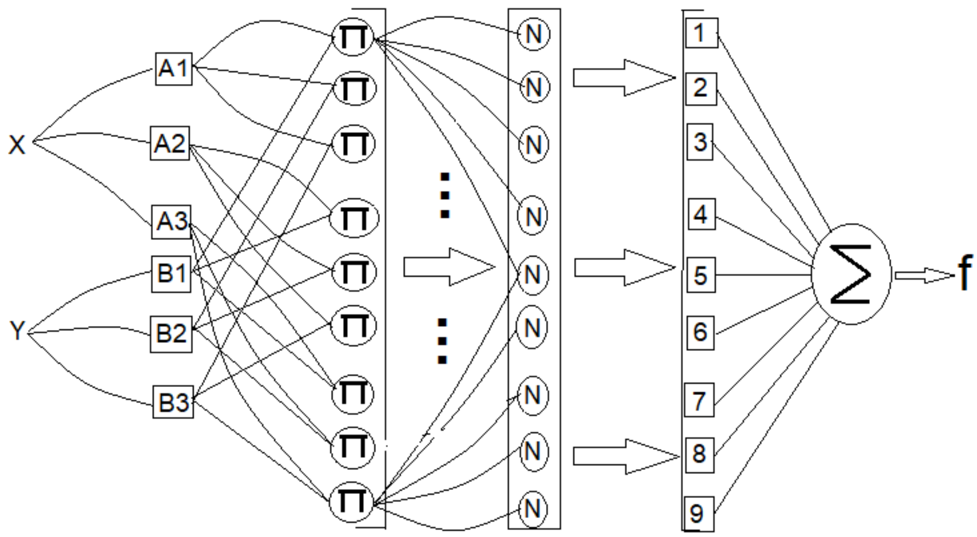


**Figure 3.** Two-input type 3 fuzzy inference.

Many researchers have studied the prediction of surface roughness using the ANFIS model with satisfactory results.

The ANFIS model has been used as a stand-alone or hybrid in CNC turning operations to forecast surface roughness [20–22]. T. Singh, P. Kumar, and J.P. Misra [23] employed ANFIS modeling to predict the surface roughness by using the Wire Electric Discharge Machining (WEDM) manufacturing method to machine the aluminum alloy AA6063. They considered four input machining variables: pulse on time (Ton), pulse off time (Toff), peak current (Ip), and servo voltage (Vs). Utilizing a scanning electron microscope (SEM), the surface integrity appearance was examined. Five alternative Ton, Toff, Ip, and Vs input parameters were used to machine the AA6063. The ANFIS was created to outperform the trapezoidal, gbell, and Gaussian membership functions with the lowest performance characteristic of the triangle membership function. M.A. Kumar [24] collected data using a CNC lathe machine by turning a stork of 50 aluminum parts with varying independent parameters: the speed, the feed, and the depth of cut. Then, the surface roughness of each part was experimentally measured. Fifty data were collected, from which 40 data were used to train the ANFIS model on the Matlab interface, while 10 data were used for testing by weighing up the performance of the bell and triangular membership functions. Furthermore, advanced regression analysis was employed in a python environment to validate the predicted outcome. As result, the ANFIS model using a bell-shaped membership function outperformed the others, with higher accuracy and a smaller error. Unlike the ANN model, the hidden layers are decided by an FIS in the ANFIS model, thus solving the well-known problem of finding the hidden layer in the ANN system to increase its prediction abilities. Despite the advantages of the ANFIS model, it has some drawbacks. Sallee et al. [25] pointed out that the burden of complexity and computing costs are two drawbacks of ANFIS that prevent it from being used in issues with extensive inputs. In order to address some of the limitations associated with ANN and ANFIS, algorithms such as genetic algorithm (GA) and particle swarm optimization (PSO) are used to train ANN and ANFIS models.

GA and PSO are optimization methods that use a fitness function to assess the population arbitrarily generated. They all use homogenous population subgrouping to enhance the quality of the solution by retarding the early clustering of the solution. GA is an approach to addressing the restricted and unrestricted optimization issues found in a biologically inspired natural process. The model alters a population of candidate solutions on a regular basis. GA arbitrarily picks people from the present population to serve as parents for the following generation's offspring during every stage. The population mutates toward an ideal solution throughout generations. PSO, on the other hand, is a computing approach to solving problems by iteratively attempting to improve a candidate solution (particle) in terms of a quality metric. It addresses the problem by generating a population (swarm) of potential solutions, referred to as particles, and shifting them about in the search space using a simple equation based on their position and velocity. PSO particles auto-update using their internal velocity rather than crossover and mutation genetics.

Despite the ANN's high success rate in handling complicated problems, Rukhaiyar et al. [26] pointed out the model's flaws, such as its sluggish learning rate. The study revealed that the PSO algorithm improves the ANN model's performance. As a result, the PSO-ANN hybrid model was developed to estimate the slope's safety factor using data obtained from 85 natural slope sections. Gopan et al. [27] used a predictive optimization algorithm combining ANN and GA. The experimental process was carried out with a silicon carbide grinding wheel on a cylindrical grinding machine. Three machining variables were chosen with three distinct ranges of speed, feed, and depth of cut. The authors used both a 3-5-1 ANN-type stand-alone and a hybrid ANN-GA model to forecast the surface roughness in a grinding operation. The results show that the ANN-GA hybrid model performs better than the ANN stand-alone model. The findings from this study demonstrate that the proposed technique might predict the grinding parameters and optimize them. ANN and GA have been employed by Hind H. Abdulridha [28] to predict the surface roughness of a mill-machined mild steel alloy. For GA, the author randomly chose the population sizes of 40, 60, and 80 at 60 iterations with a crossover percentage of 0.75 and mutation rate of 0.01. As for ANN, the author selected 2 and 10 as the numbers of hidden layers and neurons, respectively. The author also used Levenberg–Marquardt as a training function.

After exploring and studying much literature, a point to note is that researchers frequently employ soft computing models for modeling purposes in a variety of fields, including machining, but there are currently no established guidelines that may be used as a foundation for this study to create the ideal model.

In the present study, several models, ANN, ANFIS, ANN-PSO, ANN-GA, ANFIS-PSO, and ANFIS-GA, were developed to analyze the prediction of the surface roughness of aluminum Al6061. This paper proposes an approach for the prediction of surface roughness from machining parameters. Parametric analysis has been performed to fine-tune the variables within each model. Variables include the population size, the number of neurons, the membership functions, and the acceleration factors. The choice of these hyperparameters in the next section is based on their recurrence and recommendations in more pieces of literature, as described above, as well as on trial and error. A common practice in many predictions shows that they can be modified to improve the model's performance. Thiede L.A. and Parlitz U. [29] pointed out that tuning the hyperparameters becomes a crucial step in machine learning approaches because the default setting does not ensure the performance of the models. To find the ideal configuration of hyperparameters, a variety of tuning techniques, including manual search and trial and error, have been created. However, they still have to overcome these challenges. This is the particularity of the present study, where an extended number of models and hyperparameters have been considered, which brings to the study a variety of combinations that the best result is dependent on. This procedure has revealed the impact of sets of variables on the ways in which models perform. A once-for-all run of a model does not exploit its full potential to explore all possibilities to achieve the best result until the variables within the model are finely adjusted and systematically combined. Researchers and practitioners should benefit from the presentation of each strategy, together with its benefits and drawbacks, by obtaining concise yet complete information to assist them to choose the technique that best meets their needs and unique circumstances. The contribution of the present paper is to develop and analyze six different machine learning approaches and investigate how the hyperparameters affect the prediction performance of Al6061's surface roughness. This is justified by the fact that the robustness of machine learning prediction is closely related to the applications and the problems under investigation [30]. Details of the parameters and the architecture considered in the formulation of the models have been disclosed to provide clarity on the effect of the models' configuration.

## 2. Materials and Methods

Aluminum is one of the most important metals used in various industries and products, such as appliances, aviation, automotives, etc. [31]. Its chemical and mechanical properties include high ductility, high malleability, high corrosion resistance, a highly reflective surface, a low density, and its ability to be alloyed with other materials, such as zinc, copper, and magnesium. Hence, the prediction of the surface finishing would assist engineers in identifying suitable settings based on the applications. Al6061 is aluminum alloyed with magnesium and silicon as the main constituents, precipitated and hardened.

In order to investigate the link between input variable factors that identify the machine setup and output achievement or surface roughness, 30 tests were conducted. The training and testing datasets came from full-scale datasets that were made accessible and documented in the paper by I. P. Okokpujie et al. [32]. In this experiment, AL6061 material was milled using a variety of cutting dimensions and axial depths of cut, and the Press o-firm Mitutoyo surface roughness tester was employed to measure each testing result. The measurements of the surface roughness were performed 3 times and the average was taken for all 30 samples This study employed the response surface methodology to design the template used for the experiment, and, in this design, there is room for the repeatability of the samples, which permits a good optimization analysis. This study uses the response surface methodology (RSM) and the least square approximation approach to predict the surface roughness for the end-milling of an aluminum alloy machining process. The influence of numerous factors on surface roughness was examined using ANOVA, and the accuracy of the RSM forecast method was compared to that of the least square approximation forecast method. For illustration, Figure 4 shows two of 30 experimental samples of surface aluminum blocks machined at two different input settings. The 30 experimental data corresponding to the testing configurations are shown in Table 1.

**Table 1.** Experimental data.

| # | Spindle Speed (rpm) | Feed Rate (mm/min) | Axial Depth (mm) | Radial Depth (mm) |
|---|---|---|---|---|
| 1 | 1500 | 150 | 25 | 2 |
| 2 | 2500 | 150 | 25 | 2 |
| 3 | 2500 | 300 | 25 | 1 |
| 4 | 1500 | 300 | 15 | 2 |
| 5 | 1500 | 150 | 15 | 2 |
| 6 | 2000 | 200 | 20 | 2.5 |
| 7 | 1500 | 150 | 15 | 1 |
| 8 | 2000 | 200 | 20 | 1.5 |
| 9 | 1500 | 150 | 25 | 1 |
| 10 | 3000 | 200 | 20 | 1.5 |
| 11 | 2000 | 500 | 20 | 1.5 |
| 12 | 2500 | 300 | 25 | 2 |
| 13 | 2000 | 100 | 20 | 1.5 |
| 14 | 2500 | 300 | 15 | 1 |
| 15 | 2000 | 200 | 30 | 1.5 |
| 16 | 2000 | 200 | 20 | 0.5 |
| 17 | 2000 | 200 | 20 | 1.5 |
| 18 | 2500 | 150 | 15 | 2 |
| 19 | 2500 | 150 | 15 | 1 |
| 20 | 2000 | 200 | 20 | 1.5 |
| 21 | 1000 | 200 | 20 | 1.5 |
| 22 | 2500 | 300 | 15 | 2 |
| 23 | 1500 | 300 | 25 | 2 |
| 24 | 2000 | 200 | 10 | 1.5 |
| 25 | 2000 | 200 | 20 | 1.5 |
| 26 | 1500 | 300 | 15 | 1 |
| 27 | 1500 | 300 | 25 | 1 |
| 28 | 2500 | 150 | 25 | 1 |
| 29 | 2000 | 200 | 20 | 1.5 |
| 30 | 2000 | 200 | 20 | 1.5 |

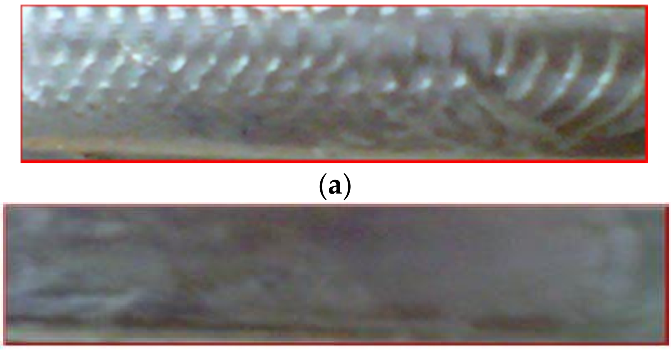

(**b**)

**Figure 4.** (**a**): Aluminum blocks—machine configuration 11: Ra = 1.16 µm (speed 2000 rpm, feed 500 mm/min, radial depth 1.5 mm, and axial depth 20 mm); (**b**) machine configuration 13: Ra = 0.5 µm (speed 2000 rpm, feed 100 mm/ min, radial depth 1.5 mm, and axial depth 20 mm).

In the present paper, the surface roughness prediction has been performed using 6 modeling approaches: ANN, ANFIS, ANN-PSO, ANN-GA, ANFIS-PSO, and ANFIS-GA. The data have been obtained from a separate study conducted by I. Okokpujie et al. [32]. The mathematical expression and mathematical models (least square approximation method and response surface methodology) have been developed to predict the surface roughness on aluminum block Al6061 alloys. These AI6061 blocks were machined on an end-milling CNC using a high-speed stainless-steel tool and minimum quantity lubrication, with results gauged using a Mitutoyo surface roughness tester and a Press o-film. This experimental study used the spindle speed, feed rate, cutting axial depth, and radial depth as controllable variables to forecast the surface finish. The obtained data have been employed to train and validate the 6 models developed using ready-made artificial intelligence models on the Matlab interface. The 6 emerging results derived from the models were compared. The best model has been considered to predict the surface roughness. Parametric analysis was performed to identify the best model layout for the system under consideration through the investigation of several configurations.

### 2.1. ANN Models

Experimental data have been used to train the ANN model and parametric analysis has been performed when varying and combining the following parameters and factors:

The network type is feedforward backpropagation;
The training function is Levenberg–Marquardt;
Three successive numbers of layers were used, namely 2, 3, and 4;
Three numbers of neurons were used, namely 10, 11, and 12.

A sigmoid function, a special tool of the logistic function to comprehend how a neural network learns to solve difficult problems, is shown in Equation (2). It is employed as an activation function in ANN. It is applied to the weighted sum of inputs in a layer and the outcome is used as input for the following layer. A neuron that uses this S-shaped function is called a sigmoid unit. It changes the model's input variables into values between 0 and 1. It makes it simple for the model to expand to a wide range of data. The variable x is calculated using Equations (3) and (4).

$$f(x) = \frac{1}{1 + \exp(-x)} \tag{2}$$

$$x = \sum_{i=1}^{m} w_{ji} u_i + \varnothing_i \text{with } j = 1 \text{ to } n \tag{3}$$

$$x = \sum_{j=1}^{m} w_{kj} u_j + \varnothing_k \text{with } k = 1 \text{ to } i \tag{4}$$

where m represents the number of input nodes; n represents the number of hidden nodes; i represents the number of output nodes; u represents the input node values; v represents the hidden node values; w is the synoptic weight, and ø is a threshold.

*2.2. ANFIS Models*

Experimental data have been used to train the ANFIS model, and parametric analysis has been performed when varying the following membership functions:

Four membership function shapes: triangular, trapezoidal, generalized bell, and Gaussian;
Two fuzzy inference system (FIS) generators: grid partition and sub-clustering;
Two optimization methods: hybrid and backpropagation.

Equations (5)–(8) briefly summarize the equations related to the membership functions considered.

- Triangular membership function (trimf): This is the most basic of various shapes. Three variables are used to determine its three points—a and c for the feet, and b for the higher vertex—as shown in Equations (5)–(8).

$$\text{Triangular}(x;\ a;\ b;\ c) = \max(\min\left(\frac{x-a}{b-a}\right), 1,\ \left(\frac{c-x}{c-d}\right), 0) \tag{5}$$

- Trapezoidal membership function (Trapmf): Its shape is defined by four scalar parameters: *a* and *b* for the feet; *c* and *d* for the sides.

$$\text{Trapezoidal}(x;\ a;\ b;\ c;\ d) = \max(\min\left(\frac{x-a}{b-a}\right), 1, \left(\frac{d-x}{d-c}\right),\ 0 \tag{6}$$

- Generalized bell-shaped membership function (Gbellmf): This is a bell-assimilated shape defined by three parameters: the curve width *a*, an integer *b*, and the center of the curve.

$$\text{Bell}(x;\ a;\ b;\ c) = \frac{1}{1 + \left|\frac{x-c}{a}\right|^{2b}} \tag{7}$$

- Gaussian membership function (Gaussmf): Unlike the above ones, the Gaussian is defined by two parameters, the curve center *c* and the curve width, as illustrated in Equation (4).

$$\text{Gaussian}(x;\ c;\ \sigma) = e^{-\frac{1\left(\frac{x-c}{\sigma}\right)^2}{2}} \tag{8}$$

$c_1$ and $c_2$ are acceleration factors;

$r_1$ and $r_2$ are two random numbers ranging between 0 and 1;

$w$ is an initial factor;

The initial population (swarm size) of size N and dimension D is given by X = [$X_1$, $X_2$, . . . , $X_N$]$^T$, with ‘T’ being the transpose operator;

Individual particle $X_p$, with $p$ = 1, 2, . . . , N, is defined as $X_p$ = [$X_{p,1}$, $X_p$,2, . . . , $X_{p,D}$];

The initial velocity of the population is defined as V = [$V_1$, $V_2$, . . . , $V_P$]$^T$;

The velocity of each particle $V_p$ with $p$ = 1, 2, . . . , N is defined as $V_p$ = [$V_{p,1}$, $V_{p,2}$, . . . , $V_{p,D}$]; the index $p$ varies from 1 to N, whereas the index q varies from 1 to D.

*2.3. ANN-PSO Model*

Experimental data have been used to train the hybrid ANN-PSO model, and parametric analysis has been performed by adjusting the following PSO factors:

Swarm size population values: 10, 20, 50, 100, 200, and 400;
Number of neurons: 5, 6, 7, 8, 9, and 10;
Acceleration factors $c_1$: 1.0, 1.5, 2.0, 2.25, 2.5;
Acceleration factors $c_2$: 2.0, 2.25, 2.5, 2.75, 3.0.

The ANN model follows the sigmoid function described in Equation (2). As for the PSO algorithm, set to optimize the ANN, Equations (9) and (10) describe the new positions of each particle in the search space. This new position is defined by the personal experience (Pbest), the overall experience (Gbest), and the actual movement of the particles.

$$V_{p,q}^{k+1} = w\ x\ V_{p,q}^{k} + c_1 r_1 \left( Pbest_{p,q}^{k} - X_{p,q}^{k} \right) + c_2 r_2 \left( Gbest_{q}^{k} - X_{p,q}^{k} \right) \tag{9}$$

$$X_{p,q}^{k+1} = X_{p,q}^{k} + V_{p,q}^{k+1} \tag{10}$$

with $Pbest_{p,q}^{k}$ representing the personal best of the $q^{\text{th}}$ component of $p^{\text{th}}$ individual, and $Gbest_{q}^{k}$ representing the $q^{\text{th}}$ component of the best individual of the population up to iteration $k$.

### *2.4. ANN-GA Model*

Experimental data have been used to train the hybrid ANN-GA model, and parametric analysis has been performed by varying the following factors:

Population size: 25, 50, 75, and 100;
Number of hidden neurons: 5 and 10.

The ANN model follows the sigmoid function described in Equation (2). As for the GA algorithm, the set to optimize the ANN is constructed following the main components: the chromosome encoding, the fitness function, selection, recombination, and the evolution scheme.

### *2.5. ANFIS-PSO Model*

Experimental data have been used to train the hybrid ANFIS-PSO model, and parametric analysis of the PSO factors has been performed by varying the following factors:

Six swarm size population values: 10, 20, 50, 100, 200, and 400;
Six neurons: 5, 6, 7, 8, 9, and 10;
Five acceleration factors $c_1$: 1.0, 1.5, 2.0, 2.25, 2.5;
Five acceleration factors $c_2$: 2.0, 2.25, 2.5, 2.75, 3.0.

### *2.6. ANFIS-GA*

Experimental data have been used to train the hybrid ANFIS-GA model, and parametric analysis has been performed by adjusting the following GA factors:

Population size values: 25, 50, 75, and 100;
Cross-over percentage: 0.4, 0.5, 0.6, 0.7, 0.8, and 0.9;
Mutation rate: 0.15 and 0.2.

The flowchart of the above study procedure is depicted in Figure 5 below.

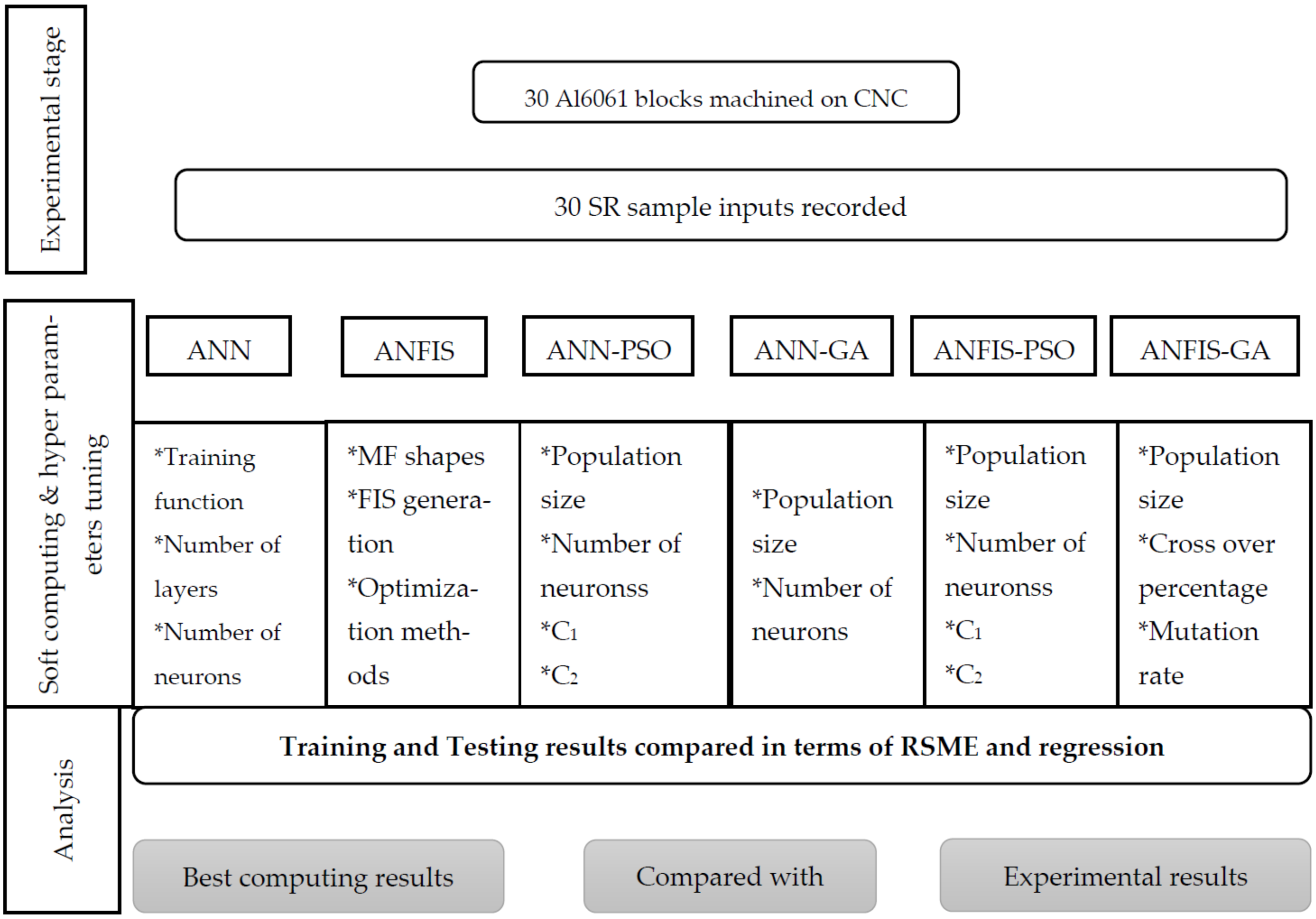


**Figure 5.** Flowchart of the study procedure.

## 3. Results

In the present section, the emerging results of each model are described and compared, and the best surface roughness prediction model is reported.

### 3.1. ANN Model

The surface roughness of machined Al6061 aluminum blocks has been predicted using the ANN model. The 30 data given in Table 1 have been employed to train the model. Here, 70% of the data have been used for training, 15% of the data used for testing, and the 15% remaining used for validation. The neural network structure describing four inputs, one hidden layer that contains 10 hidden neurons, one output layer that contains a single neuron, and one output is shown in Figure 6. The results generated by different ANN configurations are reported in Table 2 in terms of root mean square error (RMSE) and regression values ($R^2$).

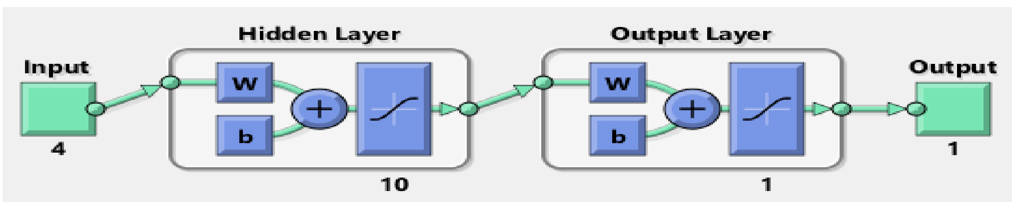


**Figure 6.** ANN structure.

**Table 2.** ANN training results.

| Number of Hidden Layers | Results (RMSE/$R^2$ Trained/$R^2$ Tested) | | |
|---|---|---|---|
| | **10 Neurons** | **11 Neurons** | **12 Neurons** |
| 1 | 0.06128/0.3538/0.7687 | 0.0518/0.8314/8466 | 0.03653/0.8587/0.9984 |
| 2 | 0.3919/0.891/0.9369 | 0.04487/0.9578/0.9396 | 0.06832/0.964/0.5667 |
| 3 | 0.0907/0.8425/0.8885 | 0.07422/0.9754/0.7466 | 0.1035/0.8919/0.8342 |

The ANN model trained and tested using the Levenberg–Marquardt training algorithm, with 12 as the number of neurons and 1 layer, has yielded better results (RMSE of 0.03653, $R^2$ of 0.8587 for training, and $R^2$ of 0.9984 for testing). Figure 7 shows the regression lines of the model, where the targets are plotted against the outputs, with both experimental and predicted mean arithmetical deviation Ra (μm).

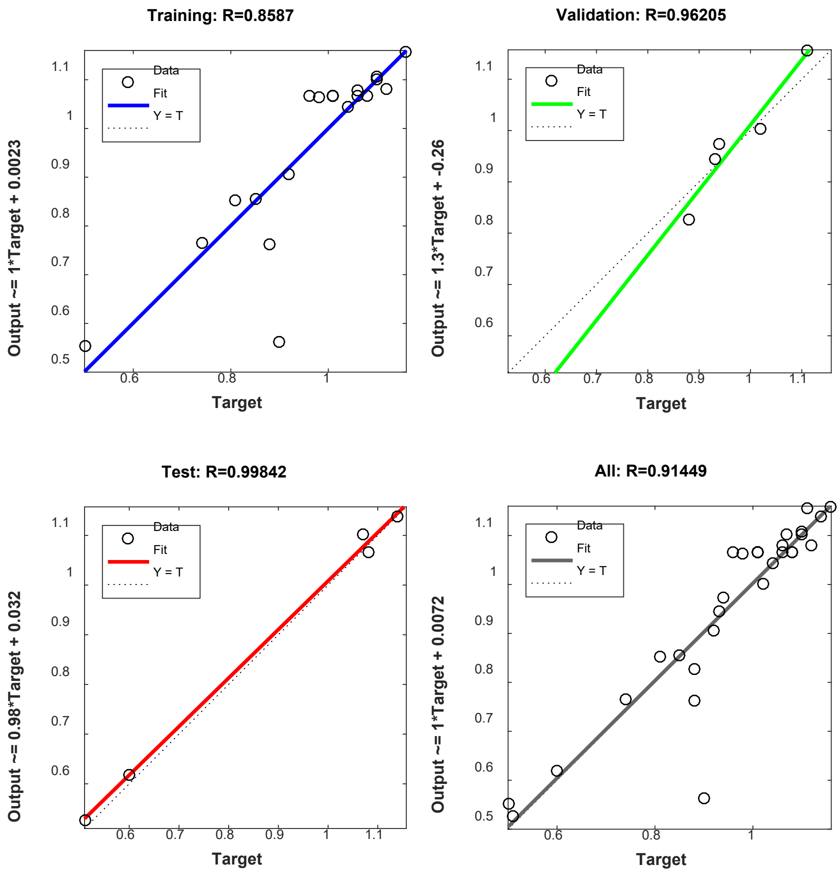


**Figure 7.** ANN regression line.

### 3.2. Adaptive Network-Based Fuzzy Inference System (ANFIS)

The surface roughness of the machined Al6061 aluminum blocks has been predicted using the ANFIS algorithm. Data in Table 1 have been employed to train the model's varying membership functions described in Section 3: membership function shapes, FIS generators, and optimization methods. In total, 24 data from the experimental results have been considered for the training, while six data have been isolated for the testing of the ANFIS model. The pictorial views of the model structure are depicted in Figure 8, and the results generated by different ANFIS configurations are recorded in Table 3 in terms of the root mean square error (RMSE) and regression values ($R^2$).

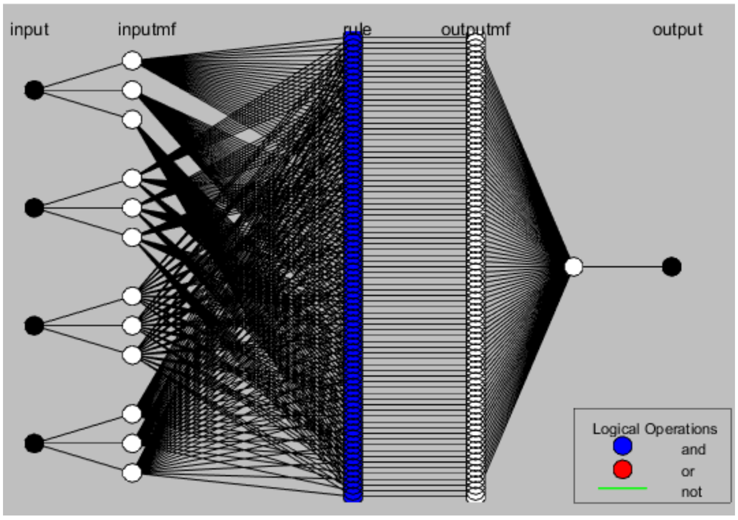


**Figure 8.** ANFIS model structure.

**Table 3.** ANFIS training results.

| FIS Generation | MF Type Input | Train FIS Opt Meth | RMSE | Training $R^2$ | Testing $R^2$ |
|---|---|---|---|---|---|
| GP | Trimf | Hybrid | 0.019105 | 0.9914 | 0.9058 |
| GP | Trapmf | Hybrid | 0.019105 | 0.7963 | 0.4917 |
| GP | gbellmf | Backprop | 0.019231 | 0.7678 | 0.4371 |
| GP | Trimf | Backprop | 0.0502853 | 0.9023 | 0.5619 |
| GP | gaussmf | Backprop | 0.0192923 | 0.8261 | 0.4567 |
| GP | Trapmf | Backprop | 0.0662746 | 0.7988 | 0.4923 |
| Sub-clust | | Hybrid | 0.0329021 | 0.7984 | 0.4866 |
| Sub-clust | | Backprop | 9.55002 | 0.7985 | 0.4921 |

The ANFIS model trained using the configuration "triangular MF shape—grid partition FIS generator—hybrid optimization method" has generated a better RMSE of 0.019105. The regression value is $R^2$ of 0.9914 for training and $R^2$ of 0.9058 for testing. Figures 9–11 show the training and testing model's regression line and the surface view, respectively, to express the ways in which inputs and output are related. Experimental data are plotted against predicted data, both expressed in terms of mean arithmetical deviation Ra (µm).

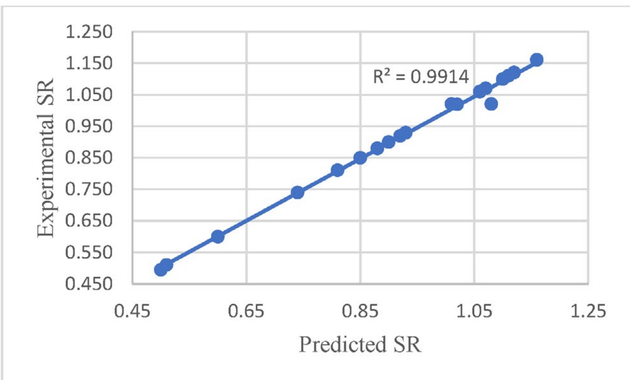


**Figure 9.** ANFIS regression line for training.

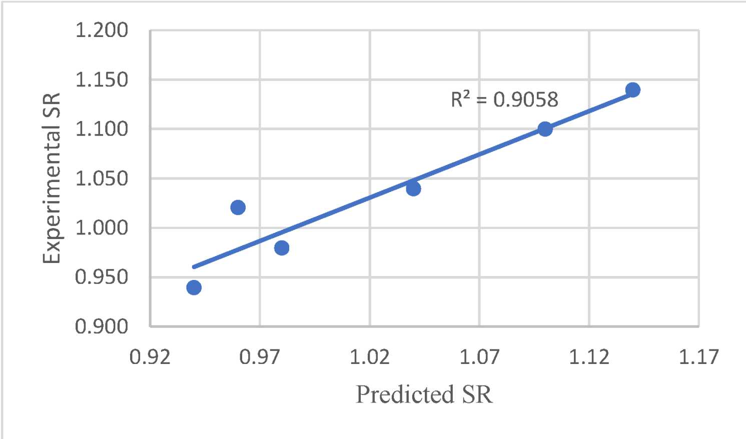


**Figure 10.** ANFIS regression line for testing.

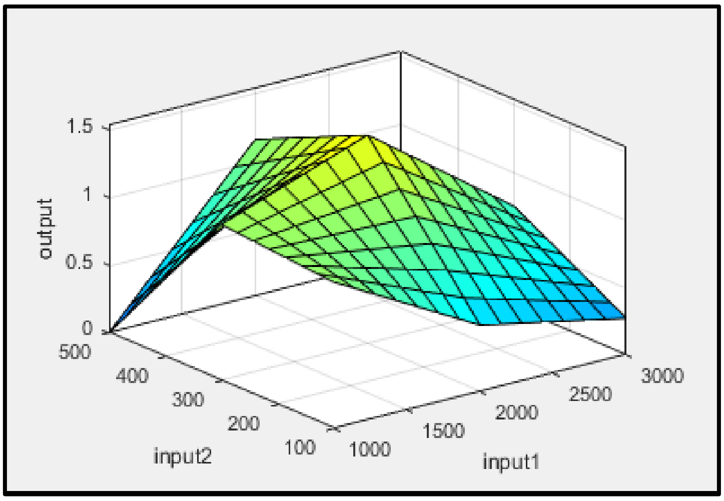


**Figure 11.** ANFIS surface view showing input 1 (Speed) and input 2 (Feed) Vs the output (SR).

### 3.3. ANN-PSO Model

The surface roughness of the machined Al6061 aluminum blocks has been predicted using the hybrid ANN-PSO model. The 30 data given in Table 1 have been employed to train the model. The feedforward backpropagation and the number of layers of two, obtained in Section 3.1, have been adopted for the model training. In total, 24 data were used for training, and six data were used for testing. The PSO-ANN parameter values considered for the sensitivity analysis in the present study are shown in Table 4. The results generated by different ANN-PSO configurations are reported in Table 5 regarding RMSE and $R^2$.

**Table 4.** Particle swarm optimization and artificial neural network parameter values.

| Population Size | Number of Neurons | Acceleration Factors | |
|---|---|---|---|
| **N** | ***n*** | $c_1$ | $c_2$ |
| 10 | 5 | | |
| 20 | 6 | 1.0 | 2.0 |
| 50 | 7 | 1.5 | 2.25 |
| 100 | 8 | 2.0 | 2.5 |
| 200 | 9 | 2.25 | 2.75 |
| 400 | 10 | 2.5 | 3.0 |

**Table 5.** Parametric results of the PSO-ANN hybrid network.

| Number | Number of Neurons (n) | Swarm Population Size (POP) | Best-Performing Acceleration Factor | | Train $R^2$ | Train MSE(10-4)/RMSE | Test $R^2$ |
|---|---|---|---|---|---|---|---|
| | | | $c_1$ | $c_2$ | | | |
| 1 | 5 | 10 | 2.25 | 2 | 0.92317 | 55/0.07416 | 0.291 |
| 2 | 5 | 20 | 2.25 | 2 | 0.95981 | 28/0.05292 | 0.7006 |
| 3 | 5 | 50 | 1.5 | 2.25 | 0.95174 | 34/0.05831 | 0.0823 |
| 4 | 5 | 100 | 1 | 2.75 | 0.96772 | 23/0.04796 | 0.1262 |
| 5 | 5 | 200 | 1.5 | 2 | 0.98079 | 14/0.03742 | 0.3716 |
| 6 | 5 | 400 | 1.5 | 2 | 0.98507 | 11/0.03317 | 0.127 |
| 7 | 6 | 10 | 1 | 3 | 0.97918 | 15/0.03873 | 0.4214 |
| 8 | 6 | 20 | 2 | 2.25 | 0.9647 | 25/0.050 | 0.2526 |
| 9 | 6 | 50 | 1 | 2.5 | 0.99201 | 5.7/0.02388 | 0.6251 |
| 10 | 6 | 100 | 1 | 2.5 | 0.98338 | 12/0.03464 | 0.7826 |
| 11 | 6 | 200 | 1 | 2.75 | 0.93273 | 47/0.06856 | 0.3446 |
| 12 | 6 | 400 | 1 | 2.25 | 0.97638 | 17/0.04123 | 0.5806 |
| 13 | 7 | 10 | 1.5 | 2.5 | 0.96297 | 27/0.05196 | 0.4519 |
| 14 | 7 | 20 | 1 | 2.75 | 0.95017 | 35/0.05916 | 0.4903 |
| 15 | 7 | 50 | 1 | 2.5 | 0.96638 | 24/0.04899 | 0.0823 |
| 16 | 7 | 100 | 1 | 2.5 | 0.99348 | 4.7/0.02168 | 0.485 |
| 17 | 7 | 200 | 1.5 | 2.25 | 0.97859 | 15/0.03873 | 0.3827 |
| 18 | 7 | 400 | 2 | 2 | 0.98933 | 7.7/0.02775 | 0.5713 |
| 19 | 8 | 10 | 1 | 2.75 | 0.98803 | 8.7/0.02950 | 0.0368 |
| 20 | 8 | 20 | 1 | 2.5 | 0.94807 | 37/0.06083 | 0.507 |
| 21 | 8 | 50 | 1.5 | 2.25 | 0.99351 | 4.7/0.02168 | 0.4674 |
| 22 | 8 | 100 | 1 | 2.5 | 0.99374 | 4.5/0.02121 | 0.2913 |
| 23 | 8 | 200 | 1 | 2.75 | 0.98494 | 11/0.03317 | 0.1764 |
| 24 | 8 | 400 | 1 | 2.25 | 0.99375 | 4.5/0.02121 | 0.2913 |
| 25 | 9 | 10 | 1 | 2.75 | 0.98066 | 14/0.03742 | 0.2203 |
| 26 | 9 | 20 | 1 | 3 | 0.98859 | 8.5/0.02916 | 0.2052 |
| 27 | 9 | 50 | 1.5 | 2.25 | 0.99345 | 4.7/0.02168 | 0.377 |
| 28 | 9 | 100 | 2 | 2 | 0.99338 | 4.8/0.02191 | 0.3081 |
| 29 | 9 | 200 | 1.5 | 2.25 | 0.9938 | 4.4/0.02098 | 0.7992 |
| 30 | 9 | 400 | 1 | 2.5 | 0.99362 | 4.6/0.02145 | 0.4983 |
| 31 | 10 | 10 | 1 | 2.75 | 0.98814 | 8.6/0.02933 | 0.6459 |
| 32 | 10 | 20 | 1.5 | 2.5 | 0.97603 | 18/0.04243 | 0.7629 |
| 33 | 10 | 50 | 1.5 | 2.5 | 0.99164 | 6.0/0.02450 | 0.2315 |
| 34 | 10 | 100 | 1 | 2.75 | 0.99295 | 5.1/0.02258 | 0.4656 |
| 35 | 10 | 200 | 1 | 2.75 | 0.99242 | 5.4/0.02324 | 0.219 |
| 36 | 10 | 400 | 1.5 | 2.5 | 0.98987 | 7.3/0.02702 | 0.3667 |

It emerged that the ANN-PSO model configuration having a population size of 200, several neurons of 9, and acceleration values $c_1$ = 1.5 and $c_2$ = 2.25 yielded a better RMSE of 0.02098, $R^2$ of 0.9938 for training, and $R^2$ of 0.7992 for testing. Figures 12 and 13 show the model's trained and tested regression lines, where the targets are plotted against the outputs, with both the experimental and predicted mean arithmetical deviation Ra (μm).

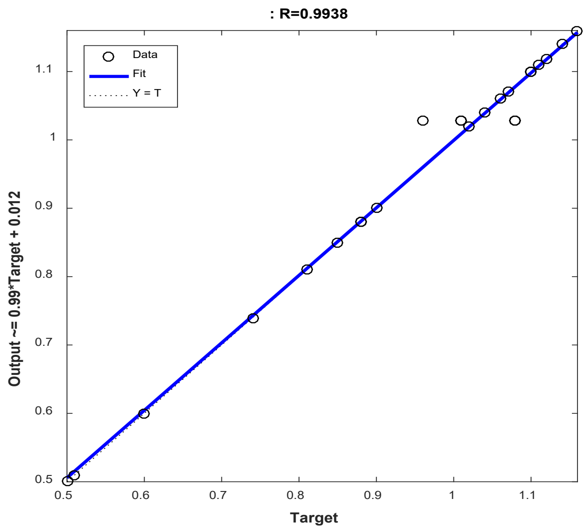


**Figure 12.** ANN-PSO regression line for training.

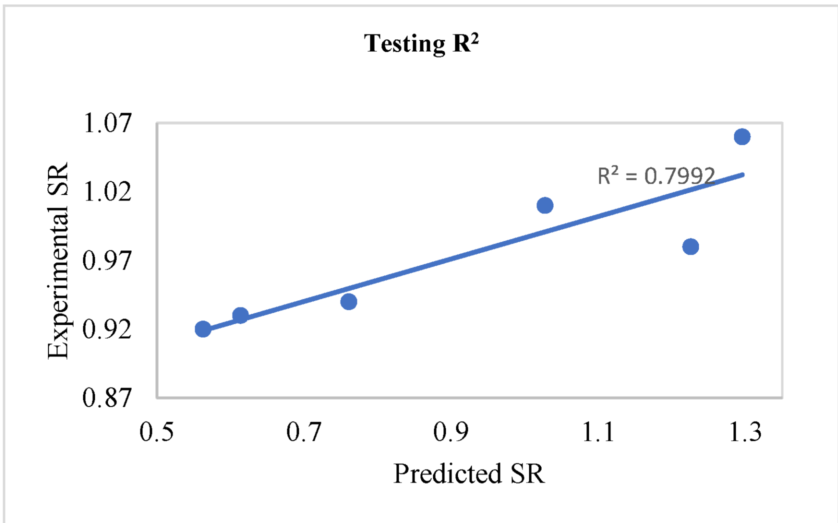


**Figure 13.** ANN-PSO regression line for testing.

*3.4. ANN-GA Model*

The surface roughness of the machined Al6061 aluminum blocks has been predicted using the hybrid ANN-GA algorithm. A total of 24 and 6 data have been, respectively, employed to train and test the model. The feedforward backpropagation and the number of layers obtained in Section 3.1 have been adopted for the actual model training. All 30 data were used for the training of the model. The results generated by different ANN-GA configurations are reported in Table 6 in terms of the root mean square error (RMSE) and regression values ($R^2$).

**Table 6.** ANN-GA training results.

| Number of Neurons | Size of Population | | | |
|---|---|---|---|---|
| | 25<br>RMSE/$R^2$ Trained<br>$R^2$ Tested | 50<br>RMSE/$R^2$ Trained<br>$R^2$ Tested | 75<br>RMSE/$R^2$ Trained<br>$R^2$ Tested | 100<br>RMSE/$R^2$ Trained<br>$R^2$ Tested |
| 5 | 0.158/0.1692<br>0.0803 | 0.156/0.2104<br>0.7669 | 0.124/0.514<br>0.8475 | 0.152/0.2487<br>0.481 |
| 10 | 0.44/0.092<br>0.3619 | 0.275/0.0358<br>0.0861 | 0.285/0.1797<br>0.000004 | 0.256/0.433<br>0.241 |

The ANN-GA hybrid model using the size of the population of 75 and number of neurons of 5 yielded better results (RMSE of 0.124 $R^2$ of 0.514 for training and 0.8475 for testing). Figures 14 and 15 show the regression lines of the training and testing models. Experimental data are plotted against predicted data, both expressed in terms of mean arithmetical deviation Ra (µm).

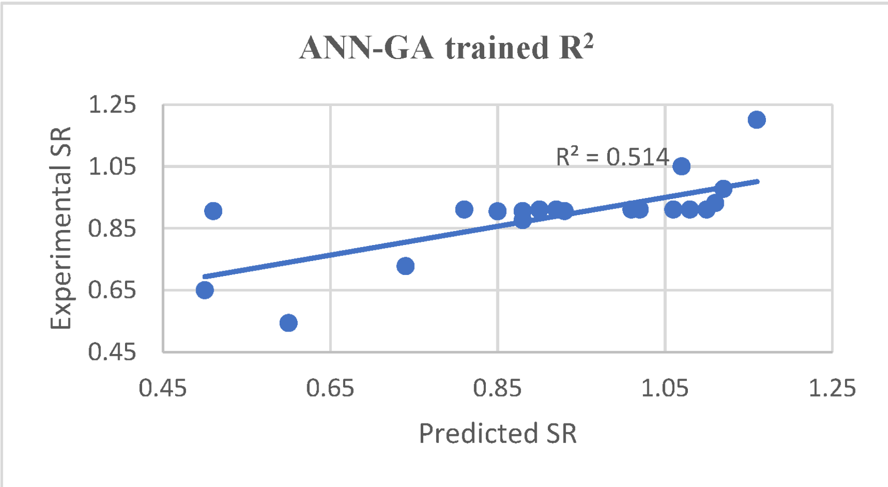


**Figure 14.** ANN-GA regression line for training.

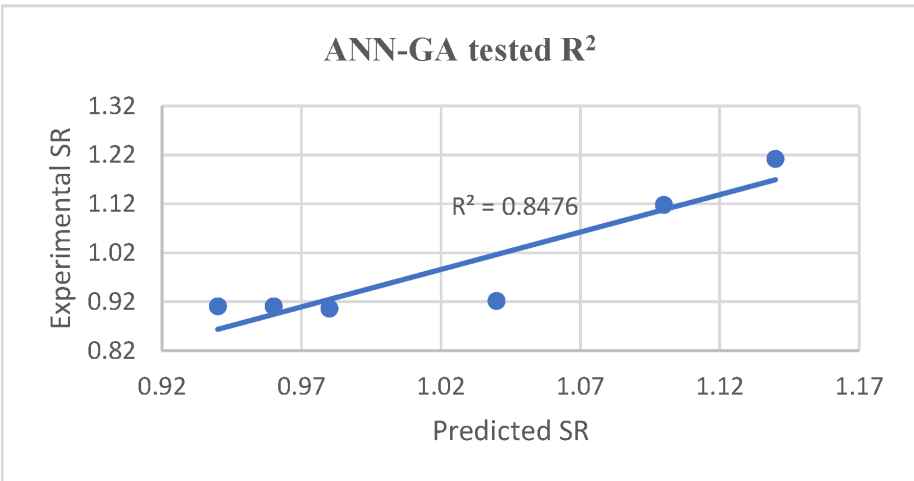


**Figure 15.** ANN-GA regression line for testing.

*3.5. ANFIS-PSO Model*

The surface roughness of the machined Al6061 aluminum blocks has been predicted using the hybrid ANFIS-PSO algorithm. A total of 21 and 9 data have been, respectively, employed to train and test the model. The swarm population size values and the acceleration factors $C_1$ and $C_2$, and the configuration "triangular MF shape—grid partition FIS generator—hybrid optimization method", reported in Section 3.2 and 3.3 have been adopted for the model training. The results generated by different ANFIS-PSO configurations are reported in Table 7 as RMSE and $R^2$.

**Table 7.** ANFIS-PSO results.

| POP | $c_1$ | $c_2$ | RMSE | $R^2$ Training/$R^2$ Testing |
|---|---|---|---|---|
| 400 | 1.0 | 2.0 | 0.0187 | 0.9484/0.016 |
| | | 2.25 | 0.02821 | 0.9533/0.8134 |
| | | 2.5 | 0.024989 | 0.9785/0.8496 |
| | | 2.75 | 0.024574 | 0.9799/0.7399 |
| | | 3.0 | 0.052431 | 0.9147/0.3561 |
| | 1.5 | 2.0 | 0.023474 | 0.9787/0.1024 |
| | | 2.25 | 0.039257 | 0.9555/0.1503 |
| | | 2.5 | 0.038532 | 0.95/0.3027 |
| | | 2.75 | 0.080054 | 0.8763/0.4759 |
| | | 3.0 | 0.053106 | 0.8492/0.6129 |
| | 2.0 | 2.0 | 0.05086 | 0.8915/0.623 |
| | | 2.25 | 0.07433 | 0.8697/0.2659 |
| | | 2.5 | 0.11021 | 0.6779/0.7602 |
| | | 2.75 | 0.082424 | 0.7561/0.4472 |
| | | 3.0 | 0.090767 | 0.5891/0.6155 |
| | 2.25 | 2.0 | 0.062678 | 0.8877/0.3566 |
| | | 2.25 | 0.098959 | 0.7556/0.3534 |
| | | 2.5 | 0.073766 | 0.7975/0.4726 |
| | | 2.75 | 0.087366 | 0.8252/0.6249 |
| | | 3.0 | 0.11701 | 0.6371/0.3199 |
| | 2.5 | 2.0 | 0.10659 | 0.6907/0.6168 |
| | | 2.25 | 0.081914 | 0.7529/0.5442 |
| | | 2.5 | 0.094932 | 0.7488/0.3495 |
| | | 2.75 | 0.1099 | 0.6476/0.5399 |
| | | 3.0 | 0.10732 | 0.6062/0.5814 |
| 200 | 1.0 | 2.0 | 0.022436 | 0.9726/0.7476 |
| | | 2.25 | 0.034272 | 0.9601/0.8235 |
| | | 2.5 | 0.045889 | 0.9401/0.856 |
| | | 2.75 | 0.047704 | 0.9193/0.2898 |
| | | 3.0 | 0.045248 | 0.8934/0.6458 |
| | 1.5 | 2.0 | 0.035986 | 0.9644/0.4331 |
| | | 2.25 | 0.044615 | 0.9438/0.3437 |
| | | 2.5 | 0.072488 | 0.8512/0.5891 |
| | | 2.75 | 0.048492 | 0.9126/0.4927 |
| | | 3.0 | 0.066796 | 0.8516/0.4622 |

**Table 7.** *Cont.*

| POP | $c_1$ | $c_2$ | RMSE | $R^2$ Training/$R^2$ Testing |
|---|---|---|---|---|
| | 2.0 | 2.0 | 0.042102 | 0.9503/0.5619 |
| | | 2.25 | 0.053739 | 0.8983/0.6719 |
| | | 2.5 | 0.048139 | 0.7162/0.2912 |
| | | 2.75 | 0.07775 | 0.7964/0.6474 |
| | | 3.0 | 0.088909 | 0.7345/0.4314 |
| | 2.25 | 2.0 | 0.048438 | 0.9217/0.317 |
| | | 2.25 | 0.08881 | 0.7832/0.6137 |
| | | 2.5 | 0.10588 | 0.7467/0.0132 |
| | | 2.75 | 0.09074 | 0.6466/0.5561 |
| | | 3.0 | 0.090626 | 0.8123/0.3778 |
| | 2.5 | 2.0 | 0.058808 | 0.8503/0.6027 |
| | | 2.25 | 0.079239 | 0.8037/0.1441 |
| | | 2.5 | 0.11467 | 0.5668/0.752 |
| | | 2.75 | 0.114020.8037 | 0.5966/0.5842 |
| | | 3.0 | 0.11955 | 0.5901/0.5279 |
| 100 | 1.0 | 2.0 | 0.028926 | 0.9712/0.0679 |
| | | 2.25 | 0.022645 | 0.9837/0.4912 |
| | | 2.5 | 0.023489 | 0.9833/0.4109 |
| | | 2.75 | 0.025881 | 0.9611/0.38 |
| | | 3 | 0.058725 | 0.9028/0.4228 |
| | 1.5 | 2.0 | 0.04066 | 0.9515/0.4741 |
| | | 2.25 | 0.040224 | 0.9291/0.4375 |
| | | 2.5 | 0.062686 | 0.7855/0.5633 |
| | | 2.75 | 0.079479 | 0.8321/0.6167 |
| | | 3.0 | 0.078211 | 0.8284/0.7792 |
| | 2.0 | 2.0 | 0.073684 | 0.8498/0.8075 |
| | | 2.25 | 0.04765 | 0.8905/0.5647 |
| | | 2.5 | 0.071991 | 0.8319/0.5242 |
| | | 2.75 | 0.10047 | 0.6368/0.4888 |
| | | 3.0 | 0.10602 | 0.6406/0.6456 |
| | 2.25 | 2.0 | 0.058442 | 0.8768/0.1513 |
| | | 2.25 | 0.10053 | 0.7394/0.7145 |
| | | 2.5 | 0.096104 | 0.7371/ 0.6162 |
| | | 2.75 | 0.096121 | 0.646/0.1097 |
| | | 3.0 | 0.10717 | 0.7317/0.787 |
| | 2.5 | 2.0 | 0.091192 | 0.7661/0.824 |
| | | 2.25 | 0.077545 | 0.815/0.2514 |
| | | 2.5 | 0.90979 | 0.6196/0.6105 |
| | | 2.75 | 0.095634 | 0.6556/0.5941 |
| | | 3.0 | 0.10024 | 0.6171/0.577 |

**Table 7.** *Cont.*

| POP | $c_1$ | $c_2$ | RMSE | $R^2$ Training/$R^2$ Testing |
|---|---|---|---|---|
| 50 | 1.0 | 2.0 | 0.04131 | 0.9351/0.416 |
| | | 2.25 | 0.01476 | 0.9923/0.8026 |
| | | 2.5 | 0.0197 | 0.9856/0.7467 |
| | | 2.75 | 0.03924 | 0.9342/0.287 |
| | | 3 | 0.054687 | 0.8867/0.4591 |
| | 1.5 | 2.0 | 0.045245 | 0.9266/0.4316 |
| | | 2.25 | 0.022922 | 0.9538/0.2011 |
| | | 2.5 | 0.056847 | 0.8958/0.5906 |
| | | 2.75 | 0.077929 | 0.8343/0.8343 |
| | | 3.0 | 0.076957 | 0.8008/0.4151 |
| | 2.0 | 2.0 | 0.044721 | 0.8967/0.0098 |
| | | 2.25 | 0.071197 | 0.8147/0.5837 |
| | | 2.5 | 0.077373 | 0.8473/0.1413 |
| | | 2.75 | 0.10129 | 0.7439/0.4286 |
| | | 3.0 | 0.077423 | 0.6865/0.5952 |
| | 2.25 | 2.0 | 0.058303 | 0.8173/0.8076 |
| | | 2.25 | 0.083255 | 0.7477/0.6418 |
| | | 2.5 | 0.087441 | 0.7232/0.3682 |
| | | 2.75 | 0.11482 | 0.6368/0.4699 |
| | | 3.0 | 0.085532 | 0.6164/0.5917 |
| | 2.5 | 2.0 | 0.091206 | 0.7648/0.6358 |
| | | 2.25 | 0.090042 | 0.6172/0.5633 |
| | | 2.5 | 0.087173 | 0.6741/0.5435 |
| | | 2.75 | 0.088626 | 0.7058/0.3009 |
| | | 3.0 | 0.099032 | 0.6889/0.6418 |
| 20 | 1.0 | 2.0 | 0.021273 | 0.9873/0.2203 |
| | | 2.25 | 0.0275 | 0.9649/0.1527 |
| | | 2.5 | 0.02423 | 0.9816/0.7212 |
| | | 2.75 | 0.032906 | 0.9656/0.4996 |
| | | 3 | 0.04202 | 0.9388/0.8849 |
| | 1.5 | 2.0 | 0.054646 | 0.8894/0.656 |
| | | 2.25 | 0.046345 | 0.9284/0.6364 |
| | | 2.5 | 0.054039 | 0.9181/0.6483 |
| | | 2.75 | 0.075662 | 0.8366/0.8086 |
| | | 3.0 | 0.097492 | 0.6866/0.2661 |
| | 2.0 | 2.0 | 0.062218 | 0.8775/0.7024 |
| | | 2.25 | 0.11006 | 0.698/0.2057 |
| | | 2.5 | 0.088353 | 0.6806/0.413 |
| | | 2.75 | 0.075375 | 0.8243/0.5263 |
| | | 3.0 | 0.1124 | 0.5894/0.6809 |

**Table 7.** *Cont.*

| POP | $c_1$ | $c_2$ | RMSE | $R^2$ Training/$R^2$ Testing |
|---|---|---|---|---|
| | 2.25 | 2.0 | 0.051421 | 0.891/0.6467 |
| | | 2.25 | 0.061426 | 0.7713/0.7581 |
| | | 2.5 | 0.081758 | 0.6605/0.5281 |
| | | 2.75 | 0.11651 | 0.5932/0.3944 |
| | | 3.0 | 0.10019 | 0.7546/0.4011 |
| | 2.5 | 2.0 | 0.070227 | 0.7341/0.6193 |
| | | 2.25 | 0.082399 | 0.775/0.0623 |
| | | 2.5 | 0.090748 | 0.6776/0.4598 |
| | | 2.75 | 0.10976 | 0.6597/0.6141 |
| | | 3.0 | 0.1172 | 0.575/0.63 |
| 10 | 1.0 | 2.0 | 0.032011 | 0.9604/0.3761 |
| | | 2.25 | 0.027135 | 0.979/0.2768 |
| | | 2.5 | 0.039251 | 0.9476/0.8061 |
| | | 2.75 | 0.049087 | 0.88/0.7045 |
| | | 3 | 0.047146 | 0.9384/0.5392 |
| | 1.5 | 2.0 | 0.059121 | 0.9137/0.19 |
| | | 2.25 | 0.060895 | 0.8911/0.4527 |
| | | 2.5 | 0.073482 | 0.8349/0.5166 |
| | | 2.75 | 0.077196 | 0.828/0.2001 |
| | | 3.0 | 0.077804 | 0.7754/0.381 |
| | 2.0 | 2.0 | 0.066434 | 0.9007/0.222 |
| | | 2.25 | 0.0755 | 0.8125/0.1046 |
| | | 2.5 | 0.082304 | 0.8261/0.6465 |
| | | 2.75 | 0.0745 | 0.6329/0.5785 |
| | | 3.0 | 0.095525 | 0.6601/0.4338 |
| | 2.25 | 2.0 | 0.072864 | 0.8064/0.5028 |
| | | 2.25 | 0.093644 | 0.7982/0.5178 |
| | | 2.5 | 0.10063 | 0.6256/0.5606 |
| | | 2.75 | 0.11651 | 0.5825/0.6127 |
| | | 3.0 | 0.055427 | 0.5786/0.723 |
| | 2.5 | 2.0 | 0.097329 | 0.715/0.646 |
| | | 2.25 | 0.075702 | 0.6745/0.5926 |
| | | 2.5 | 0.11007 | 0.6114/0.8856 |
| | | 2.75 | 0.11485 | 0.6429/0.2801 |
| | | 3.0 | 0.11423 | 0.6436/0.6004 |

It emerged that the ANFIS-PSO hybrid model having a population size of 50, the acceleration factor of $c_1$ = 1.0, and the acceleration factor of $c_2$ = 2.25 yielded better results (RMSE of 0.01476, training $R^2$ of 0.9923, and testing $R^2$ of 0.8026). In Figure 16, the prediction error and the training behavior of the ANFIS-PSO training model are plotted against the sample number.

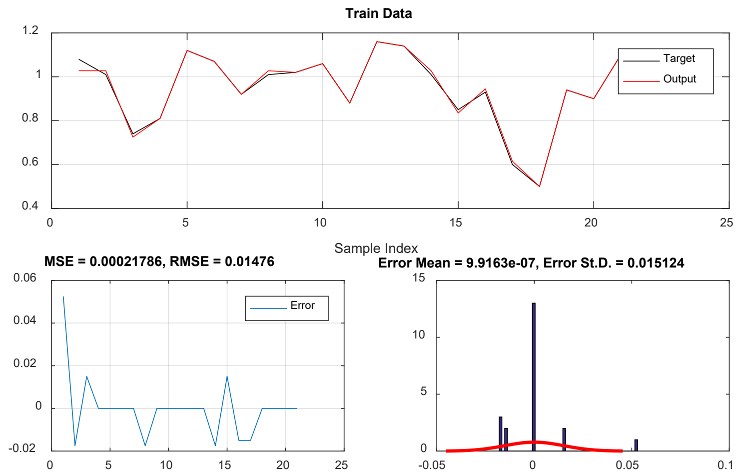


**Figure 16.** Error and training behavior of ANFIS-PSO model.

Figures 17 and 18 below show the regression lines of the ANFIS-PSO model for both training and testing. Experimental data are plotted against predicted data, both expressed in terms of mean arithmetical deviation Ra (µm).

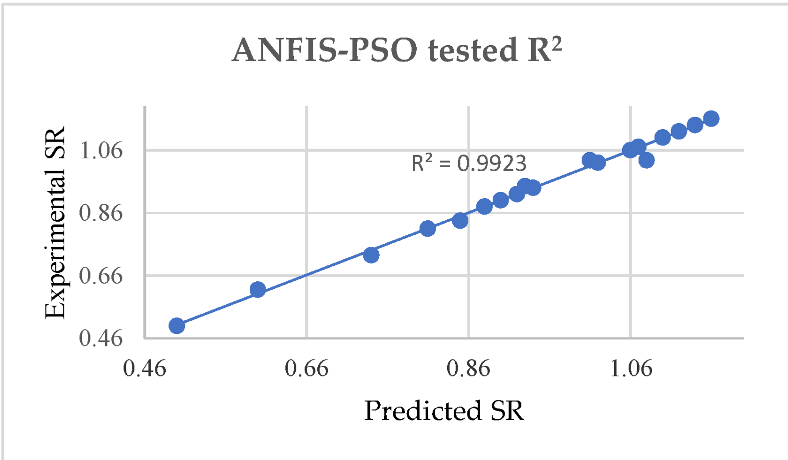


**Figure 17.** ANFIS-PSO trained regression line.

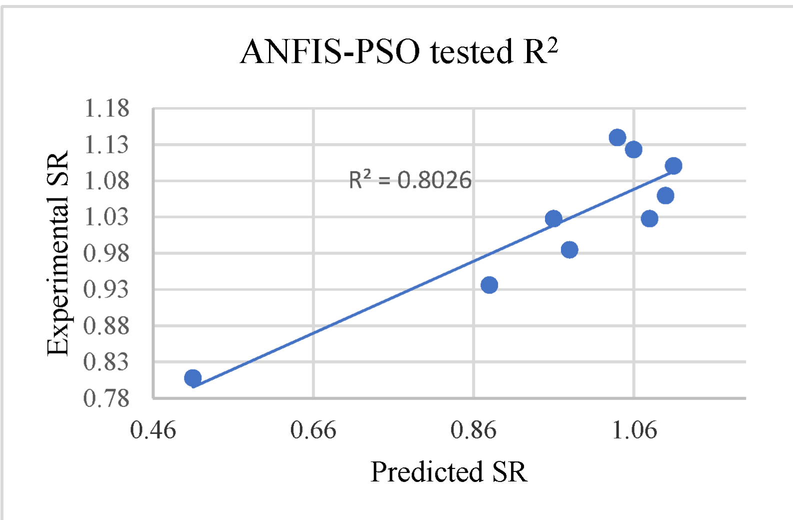


**Figure 18.** ANFIS-PSO tested regression line.

### 3.6. ANFIS-GA Model

The surface roughness of the machined Al6061 aluminum blocks has been predicted using the hybrid ANFIS-GA algorithm. A total of 23 and 7 data have been, respectively, employed to train and test the model. The swarm population size, the acceleration factors C1 and C2, and the configuration "triangular MF shape—grid partition FIS generator—hybrid optimization method" obtained in 3.2 and 3.3 have been adopted for the actual model training. The results generated by different ANFIS-GA configurations are reported in Table 8 as the RMSE value and $R^2$.

**Table 8.** ANFIS-GA training results.

| Mutation Rate | | | Cross-Over Percentage | | | | | |
|---|---|---|---|---|---|---|---|---|
| | | | **0.4** | **0.5** | **0.6** | **0.7** | **0.8** | **0.9** |
| 0.15 | POP 25 | RMSETraining | 0.023219 | 0.042373 | 0.049839 | 0.049425 | 0.03138 | 0.031286 |
| | | $R^2$ Training | 0.9717 | 0.09352 | 0.9107 | 0.8847 | 0.9573 | 0.9567 |
| | | $R^2$ Testing | 0.5657 | 0.6259 | 0.4244 | 0.4835 | 0.6113 | 0.4851 |
| | POP 50 | RMSETraining | 0.032684 | 0.032362 | 0.020916 | 0.024854 | 0.04944 | 0.054685 |
| | | $R^2$ Training | 0.9504 | 0.9102 | 0.9885 | 0.9843 | 0.8743 | 0.8954 |
| | | $R^2$ Testing | 0.4449 | 0.0184 | 0.8478 | 0.4217 | 0.7672 | 0.1663 |
| | POP 75 | RMSETraining | 0.050853 | 0.031709 | 0.052968 | 0.047598 | 0.033513 | 0.043361 |
| | | $R^2$ Training | 0.9053 | 0.9671 | 0.9083 | 0.8143 | 0.9333 | 0.9139 |
| | | $R^2$ Testing | 0.4854 | 0.0048 | 0.6328 | 0.6682 | 0.4159 | 0.7831 |
| | POP 100 | RMSETraining | 0.060105 | 0.043957 | 0.052444 | 0.049691 | 0.042643 | 0.040179 |
| | | $R^2$ Training | 0.9057 | 0.9064 | 0.9053 | 0.8649 | 0.9087 | 0.9159 |
| | | $R^2$ Testing | 0.5369 | 0.6072 | 0.0782 | 0.7063 | 0.556 | 0.7504 |
| 0.2 | POP 25 | RMSETraining | 0.010965 | 0.037879 | 0.038998 | 0.037956 | 0.032403 | 0.038689 |
| | | $R^2$ Training | 0.9939 | 0.9498 | 0.9608 | 0.9472 | 0.9404 | 0.948 |
| | | $R^2$ Testing | 0.8102 | 0.3938 | 0.6256 | 0.2204 | 0.243 | 0.5648 |
| | POP 50 | RMSETraining | 0.046424 | 0.032066 | 0.032723 | 0.03367 | 0.025307 | 0.032881 |
| | | $R^2$ Training | 0.8824 | 0.9423 | 0.9716 | 0.9699 | 0.9767 | 0.9699 |
| | | $R^2$ Testing | 0.5392 | 0.3335 | 0.1918 | 0.4859 | 0.0902 | 0.5423 |
| | POP 75 | RMSETraining | 0.055199 | 0.046364 | 0.057327 | 0.02951 | 0.033363 | 0.025371 |
| | | $R^2$ Training | 0.8934 | 0.9427 | 0.8993 | 0.9747 | 0.9698 | 0.9776 |
| | | $R^2$ Testing | 0.331 | 0.0105 | 0.6915 | 0.5921 | 0.1167 | 0.4167 |
| | POP 100 | RMSETraining | 0.052941 | 0.05037 | 0.055188 | 0.049824 | 0.036234 | 0.048645 |
| | | $R^2$ Training | 0.9308 | 0.9184 | 0.9037 | 0.9184 | 0.9588 | 0.9217 |
| | | $R^2$ Testing | 0.287 | 0.6151 | 0.5296 | 0.4995 | 0.7693 | 0.481 |

It emerged that the ANFIS-GA hybrid model trained using the size of population POP = 25, the mutation rate Mu = 0.2, and the cross-over percentage 0.4 generated a better RMSE of 0.01097 and the regression values $R^2$ of 0.9939 for training and 0.8102 for testing. In Figure 19, the prediction error and the training behavior of the ANFIS-GA training model are plotted against the sample number.

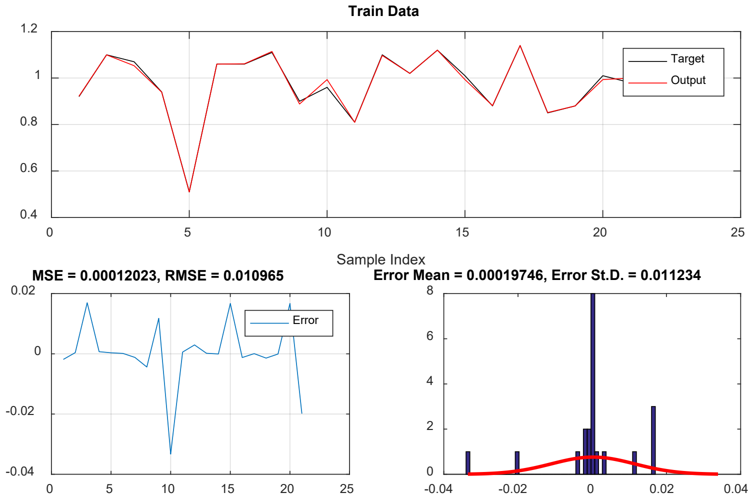


**Figure 19.** Error and training behavior of ANFIS-GA model.

Figures 20 and 21 below show the regression lines of the ANFIS-GA model for both training and testing. Experimental data are plotted against predicted data, both expressed in terms of mean arithmetical deviation Ra (μm).

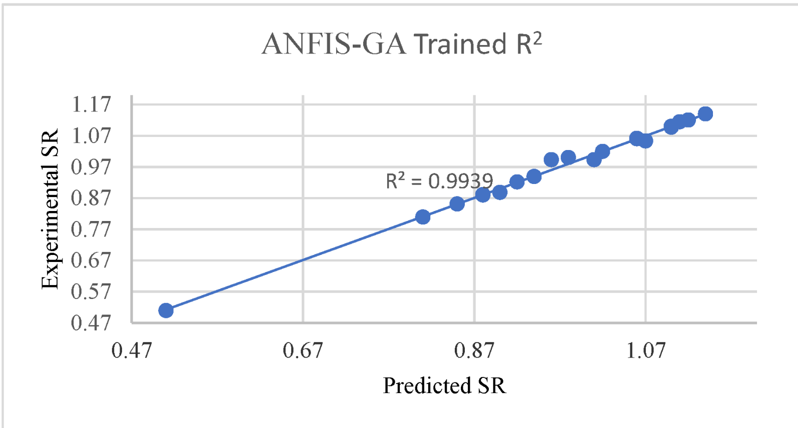


**Figure 20.** ANFIS-GA training regression line.

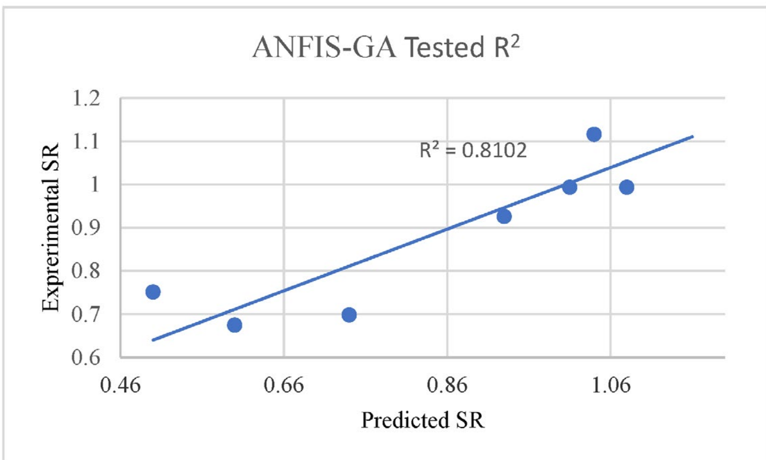


**Figure 21.** ANFIS-GA testing regression line.

### 3.7. Results Summary

After comparing the six best results emerging from the six models considered, Table 9 summarizes the emerging training results of all algorithms used in the present study to predict the surface roughness of aluminum Al6061 machined on a CNC machine. The generalization of the model, described by the testing regression value, was considered an indicator of the prediction performance. It appears that the selection of hyperparameters can potentially enhance the robustness of the models. Through the parametric analysis performed in this study, it is demonstrated that the prediction performance of the surface roughness would depend on the model configuration, which cannot be estimated a priori. It is interesting to note that ANN was the most robust approach, yielding a testing regression value of 0.9984. This can be attributed to the flexibility of the approach, which allows for the retraining and rearrangement of training and testing data to enhance the robustness of the model. This was not the case for the other proposed approach, for which testing data were selected intuitively. Nevertheless, the results revealed that the training of ANN and ANFIS with GA yields relatively higher regression values of 0.8475 and 0.8102, compared to the testing regression values of 0.7992 and 0.8026 obtained with ANN-PSO and ANFIS-PSO, respectively. Many other studies have shown same result with ANN performing better than ANFIS, but both similarly exhibiting outstanding performance in terms of accuracy [14,33,34]. Figure 22 illustrates a example of a comparison between ANFIS-GA's test results and the experimentally measured results. The testing input data of ANFIS-GA provided the following surface roughness: 0.9932, 0.9254, 0.6742, 0.7509, 0.6981, 0.9933, 0.9933, 1.2101, and 1.1160. Meanwhile, the experimental procedure yielded 1.08, 0.93, 0.6, 0.5, 0.74, 1.08, 1.01, 1.16, and 1.04. Both sets of outcome data were compared, and variances were noted and are displayed below. The largest variation was 33.4 percent, and the lowest was 0.5 percent, with roughly 90% of the resulting data falling within a 12-percentage-point range.

**Table 9.** Results summary.

| Model | RMSE | Training $R^2$ | Testing $R^2$ | Training Function |
|---|---|---|---|---|
| ANN | 0.03653 | 0.8587 | 0.9984 | Training algorithm: Levenberg–Maquardt<br>Number of layers: 1<br>Number of neurons: 12 |
| ANFIS | 0.01911 | 0.9914 | 0.9058 | Triangular MF shape<br>Grid partition FIS generator<br>Hybrid optimization method |
| ANN-PSO | 0.02098 | 0.9938 | 0.7992 | Size of the population: 200<br>Number of neurons: 9<br>Acceleration values: $c_1$ = 1.5 and $c_2$ = 2.25 |
| ANN-GA | 0.124 | 0.514 | 0.8475 | Size of the population: 75<br>Number of neurons: 5 |
| ANFIS-PSO | 0.01476 | 0.9923 | 0.8026 | Size of population: 50<br>Acceleration factors: $c_1$ = 1.0 and $c_2$ = 2.25 |
| ANFIS-GA | 0.01097 | 0.9939 | 0.8102 | Size of population: 50<br>Mutation rate (Mu): 0.2<br>Cross-over percentage: 0.4 |

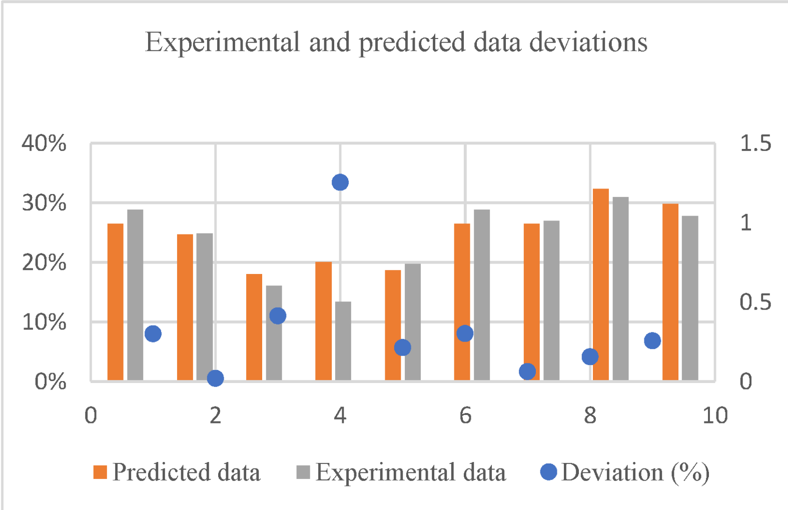


**Figure 22.** ANFIS-GA deviation graph.

## 4. Conclusions

Six algorithm models, ANN, ANFIS, ANN-PSO, ANN-GA, ANFIS-PSO, and ANFIS-GA, have been employed to predict the surface roughness of blocks of aluminum Al6061 machined on a CNC milling machine. Specific parameters, namely the spindle speed of rotation, the feed rate, and the axial and the radial depth of cut, have been used as data inputs to train the models, while the target output was the surface roughness of the machined aluminum. Parametric analysis has been performed to analyze how the hyperparameters of each model affect the prediction performance. This study reveals that an adjustment of the configuration of the models alters their robustness. Though most models exhibit a relatively higher memorization capability, as suggested by the values of the training regression, the ANN models would potentially yield the best results, based on the testing regression value. The study has shown that the effectiveness of the model being trained is heavily influenced by the hyperparameters. It highlights the impact on the quality of the model being trained. These parameters are responsible for regulating the behavior of the model and have a direct impact on its performance. The study has demonstrated that the correct selection of hyperparameters can significantly improve the overall accuracy and efficiency of the model. Thus, it is crucial for researchers and data scientists to carefully consider the hyperparameters during the training processes of models to ensure the best possible results. This study demonstrates that although soft computing techniques could potentially enhance the Al6061's surface roughness, the robustness of the models is closely related to their hyperparameters, which cannot be estimated a priori in many practical cases. The results reported in this study show that data could be used to build robust machine learning models. The robustness of these models could be enhanced through the optimization of the hyperparameters affecting their prediction performance. To strengthen the present study, our next goal is to use the predicted data results in a randomized manner during an experiment on the CNC milling machine. By doing so, we can draw a comparison between the results obtained from the predicted data and the actual experiment, which will enable us to validate the efficacy of our model. This step is crucial in ensuring that the predictions made by our model are accurate and can be relied upon for future experiments. It is our constant endeavor to improve the accuracy of our models and ensure that the results obtained are reliable and trustworthy. Through this exercise, a deeper understanding of the CNC milling machine and its behavior can be gained, which will contribute to the advancement of the manufacturing engineering field.

**Author Contributions:** Conceptualization, S.B. and L.K.T.; methodology, S.B., I.P.O. and L.K.T.; software, S.B.; validation, I.P.O. and L.K.T.; formal analysis, S.B.; investigation, S.B.; resources, L.K.T.; data curation, I.P.O.; writing—original draft preparation, S.B.; writing—review and editing, L.K.T. and I.P.O.; visualization, S.B.; supervision, L.K.T. and I.P.O.; project administration, L.K.T.; funding acquisition, L.K.T. All authors have read and agreed to the published version of the manuscript.

**Funding:** This research received no external funding.

**Institutional Review Board Statement:** Not applicable.

**Informed Consent Statement:** Not applicable.

**Data Availability Statement:** Data have been included in the paper.

**Conflicts of Interest:** The authors declare no conflict of interest.

## References

1. Burakowski, T.; Wierzchon, T. *Surface Engineering of Metals: Principles, Equipment, Technologies*; CRC Press: Boca Raton, FL, USA, 1998.
2. Lu, E.; Zhang, R.; Liu, J.; Yin, S.; Ohmori, H. Observation of ground surface roughness values obtained by stylus profilometer and white light interferometer for common metal materials. *Surf. Interface Anal.* **2022**, *54*, 587–599. [CrossRef]
3. Peta, K.; Mendak, M.; Bartkowiak, T. Discharge Energy as a Key Contributing Factor Determining Microgeometry of Aluminum Samples Created by Electrical Discharge Machining. *Crystals* **2021**, *11*, 1371. [CrossRef]
4. Okokpujie, I.P.; Okonkwo, U.C. Effects of cutting parameters on surface roughness during end milling of aluminium under minimum quantity lubrication (MQL). *Int. J. Sci. Res.* **2015**, *4*, 2937–2942.
5. Wang, S.; To, S.; Chen, X.; Chen, X. An investigation on surface finishing in ultra-precision raster milling of aluminum alloy 6061. *Proc. Inst. Mech. Eng. Part B J. Eng. Manuf.* **2015**, *229*, 1289–1301. [CrossRef]
6. Kool, J.B.; Parker, J.C.; Van Genuchten, M.T. Parameter estimation for unsaturated flow and transport models—A review. *J. Hydrol.* **1987**, *91*, 255–293. [CrossRef]
7. Subbaiah, R. A review of models for predicting soil water dynamics during trickle irrigation. *Irrig. Sci.* **2013**, *31*, 225–258. [CrossRef]
8. Weibelzahl, S.; Weber, G. Advantages, opportunities and limits of empirical evaluations: Evaluating adaptive systems. *KI* **2002**, *16*, 17–20.
9. Benardos, P.G.; Vosniakos, G.-C. Predicting surface roughness in machining: A review. *Int. J. Mach. Tools Manuf.* **2003**, *43*, 833–844. [CrossRef]
10. Boga, C.; Koroglu, T. Proper estimation of surface roughness using hybrid intelligence based on artificial neural network and genetic algorithm. *J. Manuf. Process.* **2021**, *70*, 560–569. [CrossRef]
11. Deshpande, Y.V.; Andhare, A.B.; Padole, P.M. Application of ANN to estimate surface roughness using cutting parameters, force, sound and vibration in turning of Inconel 718. *SN Appl. Sci.* **2019**, *1*, 104. [CrossRef]
12. Karabulut, Ş. Optimization of surface roughness and cutting force during AA7039/Al2O3 metal matrix composites milling using neural networks and Taguchi method. *Measurement* **2015**, *66*, 139–149. [CrossRef]
13. Baptista, D.; Morgado-Dias, F. A survey of artificial neural network training tools. *Neural. Comput. Appl.* **2013**, *23*, 609–615. [CrossRef]
14. Sada, S.O.; Ikpeseni, S.C. Evaluation of ANN and ANFIS modeling ability in the prediction of AISI 1050 steel machining performance. *Heliyon* **2021**, *7*, e06136. [CrossRef]
15. Haykin, S. *Neural Networks and Learning Machines*, 3rd ed.; Pearson Prentice Hail: Hoboken, NJ, USA, 2008.
16. Yeganefar, A.; Niknam, S.A.; Asadi, R. The use of support vector machine, neural network, and regression analysis to predict and optimize surface roughness and cutting forces in milling. *Int. J. Adv. Manuf. Technol.* **2019**, *105*, 951–965. [CrossRef]
17. Shahin, M.A.; Jaksa, M.B.; Maier, H.R. State of the art of artificial neural networks in geotechnical engineering. *Electron. J. Geotech. Eng.* **2008**, *8*, 1–26.
18. Shekhar, S.; Bera, T.C. Comparative Study of Estimated Surface Roughness Using GA and PSO Techniques for Milling of Thin-Walled Structures. In *Recent Advances in Manufacturing Modelling and Optimization*; Kumar, S., Ramkumar, J., Kyratsis, P., Eds.; Lecture Notes in Mechanical Engineering; Springer: Singapore, 2022. [CrossRef]
19. Jang, J.S. ANFIS: Adaptive-network-based fuzzy inference system. *IEEE Trans. Syst. Man Cybern.* **1993**, *3*, 665–685. [CrossRef]
20. Hweju, Z.; Abou-El-Hossein, K. Efficiency assessment of ANFIS in surface topology prediction in diamond turning of RSA443 optical aluminum using Small Datasets. *J. Phys. Conf. Ser.* **2021**, *1733*, 012012. [CrossRef]
21. Alajmi, M.S.; Almeshal, A.M. Prediction and optimization of surface roughness in a turning process using the ANFIS-QPSO method. *Materials* **2020**, *13*, 2986. [CrossRef]
22. Shivakoti, I.; Rodrigues, L.L.R.; Cep, R.; Pradhan, P.M.; Sharma, A.; Kumar Bhoi, A. Experimental Investigation and ANFIS-Based Modelling During Machining of EN31 Alloy Steel. *Materials* **2020**, *13*, 3137. [CrossRef]
23. Singh, T.; Kumar, P.; Misra, J.P. ANFIS for predicting surface roughness in wire electric discharge machining of aerospace material. *Mater. Today Proc.* **2020**, *28*, 2579–2584. [CrossRef]

24. Kumar, M.A.V. Surface Roughness Prediction Using ANFIS and Validation with Advanced Regression Algorithms. In *Intelligent and Fuzzy Techniques: Smart and Innovative Solutions*; Kahraman, C., Cevik Onar, S., Oztaysi, B., Sari, I., Cebi, S., Tolga, A., Eds.; INFUS 2020; Advances in Intelligent Systems and Computing; Springer: Cham, Switzerland, 2021; Volume 1197. [CrossRef]
25. Salleh, M.N.M.; Talpur, N.; Hussain, K. Adaptive neuro-fuzzy inference system: Overview, strengths, limitations, and solutions. In *International Conference on Data Mining and Big Data*; Springer: Cham, Switzerland, 2017; pp. 527–535.
26. Rukhaiyar, S.; Alam, M.N.; Samadhiya, N.K. A PSO-ANN hybrid model for predicting factor of safety of slope. *Int. J. Geotech. Eng.* **2018**, *12*, 556–566. [CrossRef]
27. Gopan, V.; Wins, K.L.D.; Surendran, A. Integrated ANN-GA approach for predictive modeling and optimization of grinding parameters with surface roughness as the response. *Mater. Today Proc.* **2018**, *5*, 12133–12141. [CrossRef]
28. Abdulridha, H.H. Prediction of Surface Roughness of Mild Steel Alloy in CNC Milling Process Using ANN and GA Technique. *Eng. Technol. J.* **2020**, *38*, 1842–1851. [CrossRef]
29. Thiede, L.A.; Ulrich, P. Gradient based hyperparameter optimization in Echo State Networks. *Neural Netw.* **2019**, *115*, 23–29. [CrossRef] [PubMed]
30. Gill, J.; Singh, J.; Ohunakin, O.S.; Adelekan, D.S. Artificial neural network approach for irreversibility performance analysis of domestic refrigerator by utilizing LPG with $TiO_2$–lubricant as replacement of R134a. *Int. J. Refrig.* **2018**, *89*, 159–176. [CrossRef]
31. Menzie, W.D.; Barry, J.J.; Bleiwas, D.I.; Bray, E.L.; Goonan, T.G.; Matos, G. *The Global Flow of Aluminum from 2006 through 2025*; US Department of the Interior, US Geological Survey: Reston, VA, USA, 2010.
32. Okokpujie, I.P.; Ajayi, O.O.; Afolalu, S.A.; Abioye, A.A.; Salawu, E.Y.; Udo, M. Modeling and optimization of surface roughness in end milling of aluminium using least square approximation method and response surface methodology. *Int. J. Mech. Eng. Technol. (IJMET)* **2018**, *9*, 587–600.
33. Mohanraj, T. Application of AI techniques for modeling the performance measures in milling of 7075-T6 hybrid aluminum metal matrix composites. *Int. J. Model. Simul. Sci. Comput.* **2022**, *13*, 2250034. [CrossRef]
34. Natarajan, U.; Subbaiya, P.; Anandampillai, B.; Chellamalai, M. Prediction and comparison of surface roughness in CNC-turning process by machine vision system using ANN-BP and ANFIS and ANN-DEA models. *Int. J. Mach. Mach. Mater.* **2012**, *12*, 154–177. [CrossRef]